Limnol. Oceanogr., 42(8), 1997, 1673–1684

Metabolic consequences of iron deficiency in heterotrophic marine protozoa

Z. Chase[1] *and N. M. Price*
Department of Biology, McGill University, 1205 Ave. Dr. Penfield, Montréal, Québec H3A 1B1

Abstract

Iron is recognized as a key element regulating primary production in large regions of the ocean, but nothing is known of its direct effect on higher trophic levels. Two species of heterotrophic protozoa were thus fed iron-rich and iron-poor bacterial prey and their growth and metabolism examined. Maximum growth rates of *Paraphysomonas imperforata* and *Paraphysomonas butcheri* were observed only when iron quotas of bacterial prey were >70 μmol Fe mol C^{-1}. At lower Fe : C ratios, but at constant prey biomass, both species grew significantly slower. Iron quotas of the flagellates at these slow growth rates (~10 μmol Fe mol C^{-1}) were similar to those of iron-limited phytoplankton and bacteria. Growth rate reduction was likely the result of direct, elemental limitation by iron, judging from the positive response of the protozoa to iron addition and their biochemical characteristics. Filtration and carbon ingestion rates increased under iron limitation, but gross carbon growth efficiency (GCGE) decreased when *P. imperforata* consumed iron-poor bacteria. Ammonium regeneration efficiency was also reduced. The decrease in GCGE was a consequence of reduced activity of the iron-dependent electron transport system, greater dissolved organic carbon excretion, and greater CO_2 evolution by iron-limited protozoa. *P. imperforata* excreted iron, even when limited by this element, and retained less of the ingested ration than when consuming iron-rich bacteria. Coupled with recent measurements of biogenic Fe : C in the subarctic Pacific, our results suggest that heterotrophic bacterivorous flagellates may experience iron limitation in remote oceanic regions.

Several regions of the ocean are known to be iron-limited because phytoplankton biomass increases upon addition of iron in bottle and in mesoscale fertilization experiments (e.g. Martin and Fitzwater 1988; Price et al. 1991; Martin et al. 1994; Coale et al. 1996). Research into the physiological and ecological implications of low iron availability has focused almost exclusively on the photoautotrophs. This bias reflects both the role of iron in photosynthesis and in nitrate assimilation and the importance of oceanic primary productivity in the global carbon cycle. Yet, iron is an indispensable element for growth of all aerobic organisms, and autotrophic and heterotrophic processes are tightly coupled in these iron-limited systems. Efficient grazing by microzooplankton maintains constantly low chlorophyll levels (Cullen et al. 1992; Price et al. 1994) and in general dictates the extent to which new production (Fe- or N-based) is exported and sequestered (Michaels and Silver 1988). Furthermore, grazer-mediated regeneration of iron is thought to be an important vector for the supply of dissolved Fe to phytoplankton (Barbeau et al. 1996; Hutchins et al. 1993; Hutchins and Bruland 1994). For the major nutrients, such regeneration depends on the elemental requirements of the grazers relative to the composition of their prey (Olsen et al. 1986; Caron and Goldman 1990; Sterner et al. 1992), so the same might be expected for iron. Iron limitation of secondary production could clearly have important ecological and biogeochemical consequences.

Heterotrophic metabolism depends on a respiratory electron transport system (ETS) that contains many iron-dependent redox proteins. The respiratory ETS contains ~60% more iron per mol of cytochrome-c than does the photosynthetic ETS (Raven 1988), suggesting that heterotrophs could require even more iron for growth than do phototrophs. Recently, Tortell et al. (1996) demonstrated that iron limitation of marine heterotrophic bacteria is mediated by decreased activity of the respiratory ETS. Enrichment bioassays in the Southern Ocean showed stimulation of bacterial growth, so low iron concentrations may indeed limit some heterotrophs in the sea (Pakulski et al. 1996). Because phytoplankton and bacterioplankton in iron-poor, oceanic waters contain very little iron (Sunda et al. 1991; Maldonado and Price 1996; Tortell et al. 1996), grazers in these regions may also have trouble acquiring sufficient iron for growth. Elemental limitation of heterotrophic eukaryotes (mainly freshwater zooplankton) has been considered in the cases of N and P (Hessen 1992; Urabe and Wanatabe 1992; Müller-Navarra 1995; Rothhaupt 1995), but the effect of iron content of prey on consumer metabolism has not been addressed. An increase in abundance of microheterotrophs following iron addition (Buma et al. 1991; Chavez et al. 1991; Martin et al. 1994) could represent a direct stimulation of these consumers by iron or an indirect effect caused by an increase in prey density.

Possibly the most important consumers to evaluate in the context of iron limitation are members of the protozoa. These small grazers are particularly significant in iron-limited oceanic regions (Strom and Welschmeyer 1991) where large amounts of production cycle through the microbial loop (Chavez et al. 1991). Iron in the heterotrophic bacterial biomass represents up to 50% of the total biogenic pool in

[1] Present address: Lamont-Doherty Earth Observatory, Route 9W, Palisades, New York 10964.

Acknowledgments

We thank P. Tortell for providing the bacterial C quotas and Fe : C ratios used in Table 4, M. Maldonado for useful comments throughout the study, and A. Pitts for assistance with the ETS assay. We are grateful to A. Chan and C. Suttle for providing bacterial strains, and to D. Caron for the flagellates.

This work was funded by the Natural Sciences and Engineering Research Council of Canada and the McGill University Faculty of Graduate Studies and Research. Z.C. was supported by a fellowship from the Fonds pour la Formation de Chercheurs et l'Aide à la Recherche (Québec).

the subarctic Pacific Ocean (Tortell et al. 1996) and presumably in other iron-limited waters. As the most important consumers of bacterial biomass, the protozoa thus represent a potentially significant pathway from particulate to dissolved Fe via excretion. Here we present the results of a series of laboratory experiments that demonstrate iron limitation of bactivorous flagellates and document its metabolic consequences. A simple extrapolation of these results suggests heterotrophic protists, like photoautotrophs and bacteria, may experience iron limitation in some regions of the sea.

Methods

Study organisms—Two chrysomonad microflagellates of the genus *Paraphysomonas* were examined: *P. imperforata* (clone VSI), a coastal species isolated from Vineyard Sound (Massachusetts), and *P. butcheri* (clone SS), an oceanic species from the Sargasso Sea. *P. imperforata* (4–6 μm in diam) is omnivorous and ubiquitous in marine waters (Goldman and Caron 1985). *P. butcheri* is slightly smaller (3–5 μm), but is otherwise morphologically similar to *P. imperforata.* Bacterial strains used as prey, Tef2 and Jul88, were both isolated from the Sargasso Sea on nutrient-enriched agar plates. They were maintained in batch cultures that were periodically renewed from stocks frozen in liquid nitrogen. Protozoan cultures were rendered unibacterial by repeated transfer (>10 times) into stationary-phase cultures of the prey strains (verified by microscopy).

Growth conditions and medium—The artificial seawater medium Aquil (Price et al. 1988–1989), containing the full complement of inorganic nutrients (N, P, Si), was used for all culturing and experiments. EDTA (100 μM) was used to buffer trace metals, with Cu, Mn, Zn and Co additions adjusted to achieve free-ion concentrations of $10^{-13.79}$, $10^{-8.27}$, $10^{-10.88}$, and $10^{-10.88}$ M, respectively. A total of 8.4 μM or 12.5 nM Fe was added separately as a premixed Fe-EDTA (1 : 1) complex, resulting in a pFe($-\log[Fe^{3+}]$) of 18.18 and 21.00, respectively (hereafter referred to as pFe18 and pFe21). Free metal ion concentrations were calculated by using the chemical equilibrium model MINEQL (Westall et al. 1976). Sterile medium was enriched with filter-sterilized glucose (acid-washed, 0.2-μm Acrodisc filters), which was purified of trace metal contaminants with Chelex 100 ion-exchange resin. Because carbon growth efficiency of bacteria is iron-dependent (Tortell et al. 1996), 50 and 100 mg liter^{-1} glucose were added in the pFe18 and pFe21 treatments, respectively. Such unequal concentrations yielded similar bacterial biomass in both iron treatments. At pFe18, bacteria grew at maximum rates and had high intracellular Fe quotas (iron-rich prey), whereas at pFe21, the bacteria grew slower and had low intracellular Fe quotas (iron-poor prey) (Tortell et al. 1996). When the bacteria were harvested in early stationary phase, they had consumed all of the glucose.

To minimize metal contamination, plasticware was acid-washed and then rinsed repeatedly with ultrapure water (Millipore, Q-H_2O), and all manipulations were performed in a laminar flow hood. Experimental and stock cultures of protozoa were grown at 20°C under continuous light (150 μmol quanta m^{-2} s^{-1}). Inoculations for experiments were taken from acclimated, exponentially growing stock cultures, which were transferred weekly into fresh, stationary-phase bacterial cultures (either pFe18- or pFe21-grown). Prior to the experiments with heat-killed bacteria, protozoa were repeatedly transferred into heat-killed bacterial cultures.

Overview of experiments—Initial experiments simultaneously measured the growth rate and Fe quota (μmol Fe mol C^{-1}) of *P. imperforata* fed iron-rich and iron-poor bacterial prey (strain Jul88). These experiments were repeated three times for the high-iron treatment and five times for the low-iron treatment. The quotas and growth rates of an oceanic flagellate, *P. butcheri,* were then determined under the same conditions (three times for the high-iron treatment and once for the low-iron treatment). We also examined growth of *P. imperforata* by using a second bacterial prey (Tef2), with a lower iron quota than Jul88 (Tortell et al. 1996), and tested the growth of *P. imperforata* when fed very iron-rich bacteria (strain Jul88). These last two experiments were performed only once.

Subsequent experiments focused on metabolism, using the grazer *P. imperforata* and prey Jul88. In separate experiments we measured grazer Fe and C metabolism, CO_2 evolution, ETS activity, and NH_4^+ excretion under high- and low-Fe conditions. A final experiment using "iron-coated" bacteria was designed to test biochemical vs. elemental limitation by iron. A total of five experiments were thus conducted using *P. imperforata* and Jul88, in addition to the growth and quota experiments described above.

The basic experimental approach was to grow bacterial cultures to stationary phase in pFe18 and pFe21 medium, harvest them by centrifugation (10,400 × *g*, 40 min.), and then rinse and resuspend them in a small volume of Aquil containing no trace metals, no glucose, and 100 μM EDTA as a "dissolved Fe trap" (Hutchins and Bruland 1994). This resuspension medium was referred to as Aquil-TMS (Aquil minus trace metals). Appropriate volumes of resuspended bacteria were transferred to four 250-ml polycarbonate bottles containing 200 ml of Aquil-TMS in order to achieve an initial particulate C concentration of ~2 × 10^{-7} mol ml^{-1} (~10^7 bacteria ml^{-1}). Acclimated *P. imperforata* (~10^3 cells ml^{-1}) were inoculated into two of the bottles, and the remaining bottles served as controls. Over the course of 5 d of protozoan growth, samples were periodically removed aseptically and analyzed as described below for the various experiments. Protozoa were preserved in Lugol's solution and their density measured by light microscopy in a Palmer-Maloney chamber. Deviations from this protocol are noted below.

Iron quota measurements—Doubly-labeled bacterial prey were used to measure Fe quotas (μmol Fe mol C^{-1}) of the flagellates. Bacteria were grown in the medium described above containing uniformly labeled [^{14}C]glucose (Amersham, 3 mCi mmol^{-1}) at a final activity of 2.5 μCi liter^{-1}, with either 1% (pFe18) or 10% (pFe21) of the iron as $^{55}FeCl_3$ (25–40 mCi mg^{-1}, DuPont). There was no rinsing and resuspension of prey in this experiment. When the bacteria reached stationary phase (~10^7 cells ml^{-1}), the culture was split into four bottles. Three of these were inoculated with protozoa (~10^3 cells ml^{-1}) and one served as a control. Sam-

ples for protozoan enumeration were taken every 12 h. At several intervals during middle-to-late exponential phase, 10–20 ml of culture were filtered onto 2-μm polycarbonate filters, rinsed with Ti(III) EDTA-citrate solution to remove Fe hydroxides and extracellularly bound Fe (Hudson and Morel 1989), and then rinsed twice with 5 ml of synthetic ocean water (SOW; Price et al. 1988–1989). To avoid damage to the flagellates in this and other experiments, the vacuum pressure was maintained below 50 mm Hg and the filters were not allowed to run dry prior to rinsing.

Because we used small inocula and allowed at least eight cell divisions in the labeling medium, the bacteria and protozoa had reached isotopic equilibrium at the time of sampling. Quotas were measured during that part of the protozoan growth curve where protozoan abundance was maximal and bacterial abundance minimal. At this time, bacteria represented <0.5% of the total biomass on the 2-μm filters, and protozoan retention was >95%, as determined by microscopy. Protozoan quotas were thus calculated by converting the ratio of ^{55}Fe dpm : ^{14}C dpm on the 2.0 μm filters to μmol Fe mol C^{-1} using the specific activity of C and Fe in the bacterial growth medium, after correcting for background and decay. Bacterial quotas in the control flasks were obtained similarly using 0.2-μm filters.

We tested the sensitivity of bacteria and flagellates to the Ti rinse by comparing ^{14}C activity on filters rinsed with Ti to ^{14}C activity on a subset of filters that were rinsed with an equivalent volume of SOW. We found less particulate ^{14}C activity on Ti-rinsed filters than on those that were rinsed only with SOW. The Ti rinse thus caused a small loss of labeled cellular constituents (<10% compared to SOW), but should not affect quotas measured by a dual-labeling technique.

Carbon and iron metabolism—The same doubly labeled bacterial prey described for the quota experiments were used to examine C and Fe metabolism in *P. imperforata*. Experimental and control cultures were run in duplicate. In this experiment, bacterial and protozoan densities, as well as particulate and dissolved ^{14}C and ^{55}Fe activities, were monitored at 12-h intervals over a 110-h period.

Samples for bacterial enumeration were preserved in 3.6% formalin in filtered SOW and then counted by epifluorescence microscopy (Porter and Feig 1980). Total particulate activity was determined by filtering 10–20 ml of culture onto a 0.2-μm polycarbonate filter, and then rinsing the filter twice with 5 ml of SOW. The Ti rinse was not used in this experiment because we suspected that it caused some loss of radioactivity (*see above*). Dissolved ^{55}Fe activity and dissolved organic carbon (DO^{14}C) activity were determined in 1-ml samples of 0.2-μm filtrate (Acrodisc filter with syringe) transferred to glass scintillation vials containing 100 μl of 1 N HCl. Because the medium contained high concentrations of EDTA, all of the reactive, regenerated Fe is likely to have remained in solution and not sorbed to cell surfaces and the container walls. Calculated Fe regeneration efficiencies thus represent an upper limit (Hutchins and Bruland 1994). CO_2 was allowed to purge for 24 h. During filtration, some culture was always left in the syringe so that the cells were never dry. Fluor (Ecolite) was added to all samples, and ^{14}C and ^{55}Fe activity measured by dual-label liquid scintillation counting.

CO_2 evolution—An additional experiment examined C metabolism more thoroughly. Duplicate experimental cultures and one bacterial control were used. Bacteria were grown in the [^{14}C]glucose medium described above (without ^{55}Fe), harvested, rinsed and resuspended in Aquil-TMS, and then heat-killed at 70°C for 30 min. This procedure yielded nonaggregated prey suspensions. Clumping occurred if the bacteria were heat-killed in the glucose-containing medium. The efficacy of the heat treatment was verified by inoculating aliquots of the bacterial suspension into organic-enriched seawater medium. No growth was observed. Bacterial cultures were then allowed to sit for 16 h before they were recentrifuged, resuspended in Aquil-TMS, and inoculated with *P. imperforata* as described above. In addition to measurements of DOC and particulate organic carbon (POC), CO_2 evolution was monitored directly over the time course by trapping $^{14}CO_2$ from acidified samples as described by Price and Harrison (1987). Recovery of $^{14}CO_2$ was 100%.

Calculation of metabolic parameters—Protozoan growth rate for all experiments was calculated during the exponential period by linear regression of ln(cell density) vs. time. In the C and Fe metabolism and CO_2 evolution experiments, gross growth efficiencies (GGE) for C and Fe were calculated for a time interval t, for each replicate, following Geider and Leadbeater (1988):

$$\mathrm{GGE}_x = F_{xt}/I_{xt}, \tag{1}$$

where GGE_x is the gross growth efficiency for element x, F_{xt} is the activity associated with the flagellates at time t (dpm ml^{-1}), and I_{xt} is the activity ingested by the flagellates during the interval t (dpm ml^{-1}).

More explicitly, F_{xt} was obtained after correction for bacterial biomass remaining in the bottles and caught on the 0.2-μm filter:

$$F_{xt} = P_{xt} - B_{xt}, \tag{2}$$

where P_{xt} is the total particulate (0.2-μm filter) activity (dpm ml^{-1}) and B_{xt} is the activity associated with bacteria (dpm ml^{-1}); B_{xt} = (bacteria ml^{-1}) × (^{14}C dpm or ^{55}Fe dpm bacterium^{-1}). Activity per bacterium was determined from the controls. Ingestion was calculated as

$$I_{xt} = (B_{xo} - B_{xt}) - C_I, \tag{3}$$

where B_{xo} and B_{xt} represent the bacterial activity (^{14}C or ^{55}Fe) in the flagellate bottle at the beginning and end of the interval, respectively, and C_I is a correction for loss of particulate activity in the controls (*see below*). Time t was taken from the beginning of exponential growth of the flagellates until their peak in biomass, as determined from inspection of the growth curve. Because the flagellates had essentially not consumed any bacteria at the beginning of this interval, all the activity at this time was associated with the bacteria, and B_{xo} was taken to be the total initial particulate activity. Release of an element to the dissolved phase, E_{xt}, was calculated as

$$E_{xt} = (D_{xt} - D_{xo}) - C_E, \tag{4}$$

where D_{xt} and D_{xo} represent dissolved activity in the flagellate bottle at the end and beginning of the interval, respectively.

Where necessary, a correction (C_E) was applied to account for directional changes in control cultures. This was obtained by multiplying the change in dissolved activity/bacterium in the controls (con) by the logarithmic mean number of bacteria in the flagellate bottles (exp) during interval t. C_I was calculated similarly from particulate activity in the controls; that is,

$$C_{E,I} = [|A_t - A_0|/(\text{bacteria ml}^{-1})]_{\text{con}} \times (\text{bacteria ml}^{-1})_{\text{exp}}, \quad (5)$$

where A refers to dissolved or particulate activity in the controls, yielding C_E and C_I, respectively. For comparative purposes, F_{xt} (growth), I_{xt} (ingestion), and E_{xt} (excretion) were converted to mol protozoan^{-1} d^{-1} by dividing by the specific activity (SA) of the bacteria (dpm mol^{-1} Fe or C), the logarithmic mean number of protozoa during the interval, and the duration of the interval. Rates were converted to regeneration efficiencies (RE) by normalizing to the quantity of the element ingested during the same period:

$$\text{RE}_x = E_{xt}/I_{xt}. \quad (6)$$

Elemental content of the flagellates (mol protozoan^{-1}) was obtained by dividing F_{xt}/SA by the number of flagellates ml^{-1} at time t. Unless otherwise noted, all the data reported represent means ±1 SD.

Electron transport system (ETS) activity—Heat-killed, iron-rich and iron-poor prey were prepared as described above. Duplicate experimental cultures and one bacterial control were used. During the exponential phase, duplicate samples of 35 ml were gently filtered onto combusted (425°C for 4 h) Whatman GF/C filters. ETS activity was measured according to Packard and Williams (1981), except samples were homogenized with a Mini Bead Beater (Xymotech). Tetrazolium (INT) reduction rates were converted to rates of O_2 consumption by using the extinction coefficient for INT-formazan reported by Kenner and Ahmed (1975). We normalized ETS activity to cell density and to protein concentration in each sample, determined using the fluorescamine method of Udenfriend et al. (1972).

NH_4^+ excretion—Ammonium excretion by *P. imperforata* was monitored in a grazing experiment with iron-rich and iron-poor ^{14}C-labeled prey. Duplicate experimental cultures and one bacterial control were used. In this experiment, bacteria were inhibited by UV irradiation. This treatment was used initially in our study before we had overcome the problem of clumping in heat-killed cultures (*see above*). Bacterial cultures were transferred to plastic beakers covered with cellophane and irradiated with a 30 W germicidal bulb four times for 5 min, with gentle mixing between exposures. Cultures were then centrifuged and treated in the same manner as for the other experiments. UV irradiation inhibited bacterial replication, but not respiration. Ammonium concentrations in 0.2-μm filtrate were measured by the method described by Parsons et al. (1984). In control cultures, which contained UV-irradiated bacteria without flagellates, NH_4^+ concentration did not change over time. Experimental bottles were corrected for this constant background concentration. Carbon ingestion rates were calculated by the disappearance of ^{14}C activity, as described above. Ammonium excretion rates were calculated by dividing the slope of the excretion curve (mol ml^{-1} h^{-1}) by the logarithmic mean number of protozoa. Rates were expressed as regeneration efficiencies—(NH_4^+ excreted/N ingested) × 100—by converting C ingested to N ingested using the previously published C:N ratio for strain Jul88. This ratio was the same in iron-sufficient and iron-deficient bacteria (3.4 ± 0.7 and 3.9 ± 0.3 mol C mol N^{-1}, respectively; Tortell et al. 1996).

Table 1. Iron quotas of *Paraphysomonas* spp. grown with bacterial prey that were cultured under high- and low-iron conditions (pFe18 and pFe2 medium, respectively). In each experiment, protozoan quotas were obtained from triplicate cultures and bacterial quotas were obtained from one control culture. Values represent means of all experiments ± SE, calculated by error propagation, and n refers to the number of independent experiments.

	Fe:C (μmol Fe mol C^{-1})			
	High iron	n	Low iron	n
Bacterial prey (strain Jul88)	103±5	6	5.8±0.1	6
P. butcheri	101±12	3	12.5±0.2	1
P. imperforata	98±3	3	8.2±0.1	5

Biochemical vs. elemental limitation—A culture of Jul88 was grown to stationary phase in pFe21 medium, heat-killed, rinsed once, and resuspended in Aquil-TMS. The culture was then divided equally into two centrifuge bottles, one of which was enriched with 8.4 μM Fe-EDTA. After 2 h, both cultures were harvested, resuspended in Aquil-TMS, split in two, and inoculated with acclimated *P. imperforata*. A preliminary investigation of the kinetics of ^{55}Fe adsorption by dead bacteria demonstrated that the added iron was rapidly scavenged onto the cell surfaces. By comparing the ^{55}Fe activity of Ti-rinsed and SOW-rinsed bacteria in this experiment, we determined that about 20 amol Fe cell^{-1} was bound extracellularly, roughly 10 times more than the intracellular iron content of iron-deplete bacteria.

Results

Growth and quotas—P. imperforata grew significantly slower (by 44%; $P < 0.005$) and achieved lower levels of biomass when consuming iron-poor as opposed to iron-rich prey (μ = 2.52 ± 0.08 d^{-1}, n = 3 for pFe18; μ = 1.4 ± 0.1 d^{-1}, n = 5 for pFe21). The high- and low-iron bacterial quotas that elicited this growth response are reported in Table 1. Indeed, over a wider range of bacterial Fe:C and initial particulate Fe in the medium, protozoan growth increased with the iron content of prey items (Fig. 1). Reduction in growth was observed for both species of protozoa and for *P. imperforata* fed Tef2 or Jul88 (Fig. 1). Small differences in initial bacterial C biomass in these experiments could not account for the growth response (Pearson product-moment correlation, P = 0.241), nor was bacterial Fe:C related to total particulate C (mol C ml^{-1}) (Pearson product-moment correlation, P = 0.226). Maximum growth rates of the protozoa were observed only at bacterial Fe:C ratios >70 μmol mol^{-1}, and growth rates at low and high

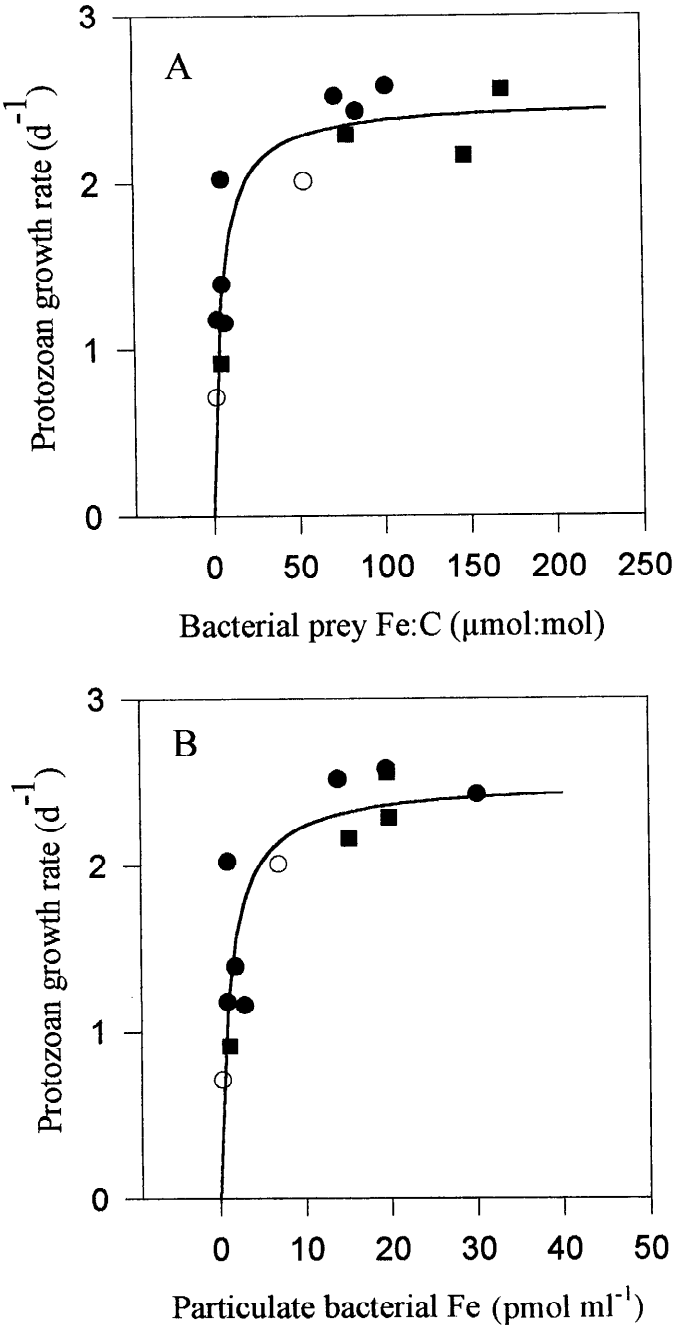

Fig. 1. Protozoan growth rates (d^{-1}) in batch culture as a function of (A) prey iron quota (μmol Fe mol C^{-1}) and (B) the initial concentration of particulate Fe (○), *Paraphysomonas butcheri* growing on strain Jul88 (■), and *Paraphysomonas imperforata* growing on strain Jul88 (●), and strain Tef2 (○). Initial bacterial biomass ranged from 1 to 4 × 10^{-7} mol C ml^{-1}, or 2.2 to 16 × 10^7 cells ml^{-1} (the high cell densities are for Tef 2, which has a C quota of ~7 × 10^{-15} mol Fe $cell^{-1}$; P. Tortell unpubl.), and was independent of the Fe:C ratio. Differences in bacterial Fe:C were obtained by altering medium chemistry and, for the very high quotas, by allowing the bacteria to starve. Mean growth rates are based on replicates that differed by <5% on average. The curves were fitted to the Michaelis–Menton equation by nonlinear regression. A. μ_{max} = 2.48 d^{-1} and K_m = 4.60 μmol Fe mol C^{-1}, r^2 = 0.82. B. μ_{max} = 2.50 d^{-1} and K_m = 1.16 pmol Fe ml^{-1}, r^2 = 0.73.

iron were independent of bacterial prey species (Fig. 1). Similar rates of slow growth were observed when protozoa were inoculated into cultures of iron-poor bacteria that were in stationary phase or that were rinsed and resuspended in iron-free medium (data not shown). Because the stationary bacterial cultures contained ~8 nM of iron complexed to EDTA, the flagellates were apparently unable to use such low concentrations of dissolved Fe directly for growth.

Under low-iron conditions, Fe quotas (μmol Fe mol C^{-1}) of both species decreased to about a tenth of their maximum values and were significantly ($P < 0.005$) higher in the oceanic (*P. butcheri*) than in the coastal isolate (*P. imperforata*) (Table 1). These low Fe quotas are at the high end of those reported for a number of iron-limited phytoplankton (0.7–14; Maldonado and Price 1996) and heterotrophic bacteria (2.3–14; Tortell et al. 1996). Iron quotas of both flagellates were significantly higher than those of their prey at low iron ($P < 0.005$).

To test whether the observed growth inhibition was a direct consequence of mineral iron limitation or an indirect effect of secondary (biochemical or morphological) differences between iron-rich and iron-poor bacterial prey, we increased the iron content of heat-killed, iron-poor bacteria by briefly exposing them to high concentrations of dissolved Fe. *P. imperforata* grew significantly ($P < 0.01$) faster when consuming these iron-coated, biochemically iron-deficient bacteria (3.21 ± 0.04 d^{-1}) than when consuming the standard iron-poor prey (2.59 ± 0.08 d^{-1}). Inexplicably, the growth of *P. imperforata* was unusually fast in both treatments of this experiment (cf. Fig. 1).

A number of grazing experiments were performed with *P. imperforata* to determine the metabolic consequences of iron limitation. For these trials we used pFe18- and pFe21-grown bacterial prey (Jul88) as the iron-rich and iron-poor treatments (mean quotas reported in Table 1). The first experiment examined C and Fe metabolism using dual-labeled prey. While the protozoa grazed the bacterial prey and increased in number (Fig. 2), particulate C decreased by 57 and 83% in the pFe18 and pFe21 treatments, respectively (Fig. 3), and particulate Fe decreased by 70 and 85% in the same bottles (Fig. 4). A concomitant appearance of DOC (Fig. 3) and dissolved Fe (Fig. 4) occurred in the bottles inoculated with protozoa. Control bottles containing only bacteria resuspended in carbon-free medium showed little or no change in the particulate or dissolved fraction of either C or Fe. Bacterial density in the controls did not change over the course of the experiment (data not shown).

Carbon metabolism—The reduced growth rate of protozoa fed the iron-poor diet (Fig. 1) was not a consequence of their slower ingestion rates, as they consumed more bacterial C than did those fed iron-rich prey (Table 2). The ingestion rates corresponded to filtration rates of 26.41 ± 0.09 and 60.0 ± 0.6 nl $protozoan^{-1}$ d^{-1} for pFe18 and pFe21, respectively, similar to maximum rates observed for other bacterivorous flagellates (Caron et al. 1985). Initial bacterial density was comparable in the two iron treatments (Fig. 2; 5.9 ± 0.9 and 6.85 ± 0.07 × 10^7 cells ml^{-1} for pFe18 and pFe21, respectively). The calculated bacterial C quota, based on this initial sampling point, was slightly higher in the iron-

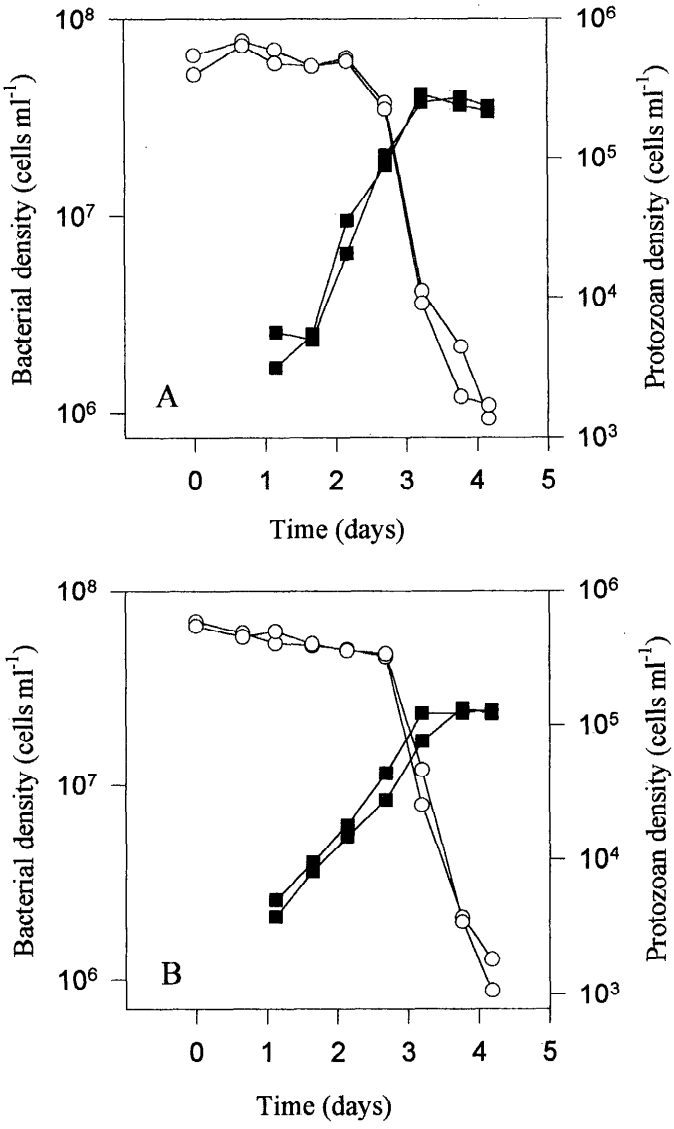

Fig. 2. Growth of *Paraphysomonas imperforata* (■) and concomitant decrease in prey Jul88 abundance (○) in replicate batch cultures during the C and Fe metabolism experiment. A. Iron-rich bacteria (pFe18-grown); μ = 2.5 ± 0.1 d^{-1}. B. Iron-poor bacteria (pFe21-grown); μ = 1.4 ± 0.2 d^{-1}.

poor bacteria (3.3 ± 0.2 and 4.3 ± 0.4 fmol C cell^{-1} from duplicate pFe18 and pFe21 cultures). However, by using all available data, including control cultures in all experiments at all sampling times, we found no differences in the C quota of the bacterial prey as a function of iron status (4.2 ± 0.3 and 4.4 ± 0.4 fmol C cell^{-1}; mean ± SE of pFe18 and pFe21 cultures; all data, n = 30 and 20, respectively). Thus, the difference in filtration rate was not likely a result of a difference in C content of the prey. The C quota of *P. imperforata* was similarly not affected by iron status (0.243 ± 0.005 and 0.245 ± 0.005 pmol C cell^{-1}; mean ± SE of high and low-iron cultures; n = 14 and 10, respectively).

Excretion of DOC (pmol C protozoan^{-1} d^{-1}) was greater by iron-limited than by iron-sufficient protozoa, even when normalized to their faster ingestion rates, resulting in a lower C assimilation efficiency (CAE) ($P < 0.025$) (Table 2). Gross carbon growth efficiency (GCGE) of the flagellates was also lower in the low-iron treatment. This decrease in GCGE, however, could not be accounted for solely by the difference in CAE. Mass-balance calculations for the experiment with live prey suggested the decrease in GCGE was also due to greater CO_2 evolution by the iron-limited protozoa (Table 2). This result was confirmed in a separate experiment using heat-killed bacterial prey where $^{14}CO_2$ evolution was measured directly. Thus, in the low-iron treatment, *P. imperforata* released significantly more ingested bacterial C as CO_2 (Table 2; $P < 0.025$). In both replicates of both iron treatments there was no change in the total amount of C measured over the course of the experiment, despite major shifts in the relative contribution of each pool. Thus, all C pools were quantitatively recovered by our methods, with no systematic losses.

Initial prey C biomass was lower in the CO_2 experiment than in the C and Fe metabolism experiment using doubly labeled prey, but the calculated metabolic parameters from both experiments were similar (Table 2). Because the bacterial densities were high relative to natural abundances and were likely above saturation (e.g. Fenchel 1982), we think protozoan metabolic parameters and growth were insensitive to the relatively small differences in initial prey density among experiments and between iron treatments.

Iron-limited protozoa released more CO_2, but they did not have greater respiration rates (O_2 consumption), according to the measurements of ETS activity. In fact, the activity of the iron-dependent ETS decreased 10-fold when *P. imperforata* was fed iron-poor compared to iron-rich prey (from 4 ± 1 to 0.36 ± 0.06 pmol O_2 protozoan^{-1} d^{-1} in pFe18 and pFe21 cultures). This result was not due to differential retention of flagellates on GF/C filters, as the same trend was observed when ETS activity was normalized to the total protein of each sample (182 ± 51 and 39 ± 10 mmol O_2 g protein^{-1} d^{-1} in pFe18 and pFe21 cultures).

Nitrogen metabolism—Absolute rates of NH_4^+ excretion by exponential-phase *P. imperforata* were not affected by iron nutritional status (0.24 ± 0.01 and 0.233 ± 0.005 pmol NH_4^+ flagellate^{-1} d^{-1} for iron-sufficient and iron-deficient cells, respectively), but NH_4^+ regeneration efficiency of iron-sufficient protozoa (24.4 ± 0.8%) was significantly higher than that of iron-deficient cells (15.3 ± 0.8%; t-test, $P < 0.05$).

Iron metabolism—We calculated an iron budget (Table 3) for *P. imperforata* using the iron data from the dual-label experiment (Fig. 4). Surprisingly, the iron-limited protozoa excreted more of the ingested iron than did protozoa consuming iron-rich prey, and thus they had a lower gross Fe growth efficiency (GFeGE) (Table 3). In the low-iron experiment, the amount of iron excreted and sequestered (14 ± 2 amol Fe protozoan^{-1} d^{-1}) during protozoan growth equalled the amount of iron ingested (16 ± 2 amol Fe protozoan^{-1} d^{-1}), as it should for mass balance (t-test, $P > 0.05$). In the high-iron experiment, slightly more iron was ingested on average (110 ± 7 amol Fe protozoan^{-1} d^{-1}) than

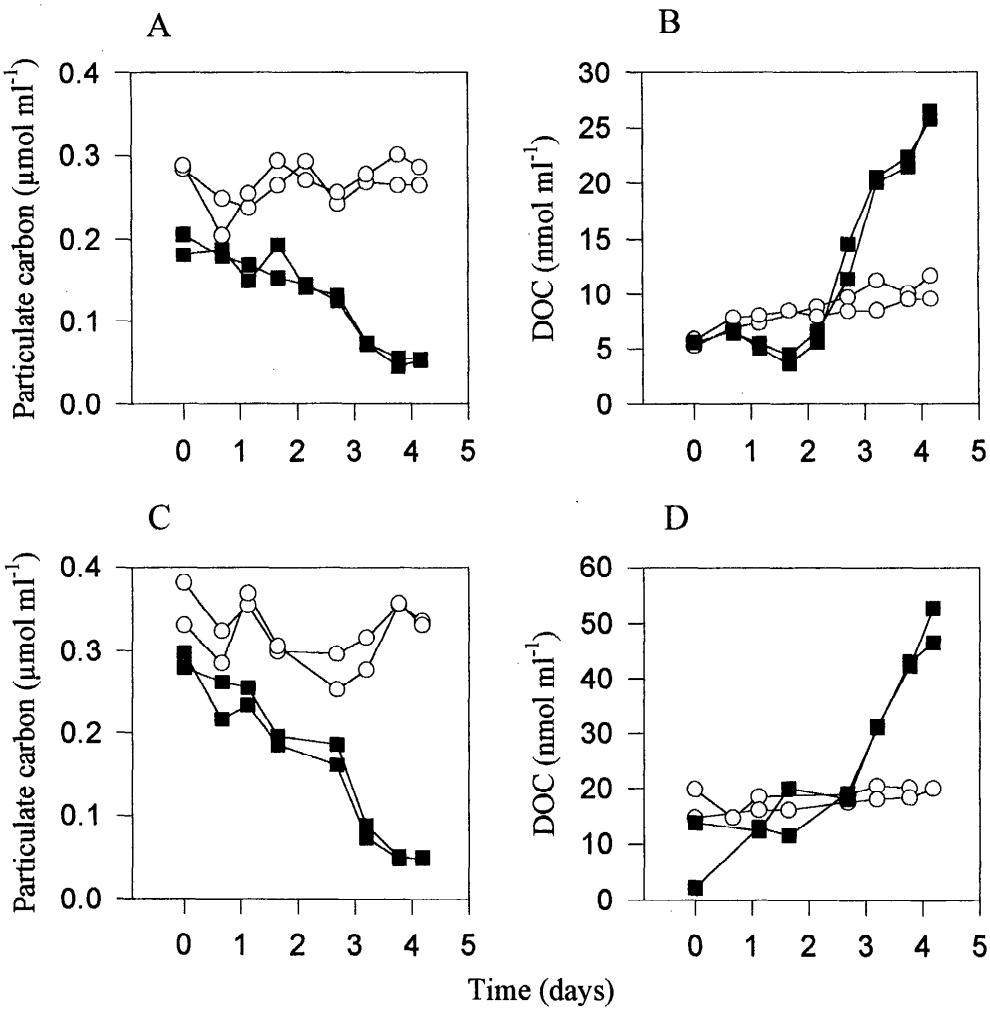

Fig. 3. Time course of carbon dynamics in cultures with bacteria and *Paraphysomonas imperforata* (■; replicates shown) and control cultures with bacteria alone (○; replicates shown). Particulate (POC) (A) and dissolved (DOC) (B) organic carbon in the high-iron (Fe-rich bacteria) treatment. POC (C) and DOC (D) in the low-iron (Fe-poor bacteria) treatment.

could be accounted for by growth and excretion (92 ± 6.3 amol Fe protozoan^{-1} d^{-1}), but the discrepancy was small and not statistically significant (*t*-test, $P > 0.05$). As observed for C, the total amount of iron (particulate + dissolved) recovered over the course of the experiment was constant, so we are fairly confident that all iron pools were recovered quantitatively. Furthermore, although wall loss was not assessed directly in these experiments, we assume it was minimal in the presence of EDTA, which served as a "dissolved trap" for regenerated Fe and prevented adsorption to cell surfaces and the sides of incubation bottles (Hutchins and Bruland 1994). When the same experiment was performed without the addition of 100 μM EDTA, iron regeneration efficiencies for both treatments were ~80% less than those observed in the presence of EDTA, suggesting that a large amount of the regenerated Fe was reactive toward cell and bottle surfaces. Samples used to calculate the iron metabolic parameters were rinsed only with SOW, not with Ti. The ingested fraction thus included any Ti-labile Fe on the surface of the bacterial prey. However, comparison of Fe:C ratios on a subset of the control and experimental samples washed with both Ti-citrate reagent and SOW revealed that very little iron (~10%, pFe18; <1%, pFe21) was bound to cell-surface ligands. The process of rinsing and resuspending the prey cells in Aquil containing 100 μM EDTA (Aquil-TMS, *see* methods) was apparently sufficient to remove what little surface-bound Fe was present.

Discussion

Growth rate—P. imperforata and *P. butcheri* were unable to achieve maximum growth rates when consuming iron-poor bacteria, and *P. imperforata* was inhibited regardless of which bacterial stain was offered as prey (*see Fig. 1*). Although these data form a rather piecemeal functional response with a composite half-saturation constant of 4.6 μmol Fe mol C^{-1}, they show clearly that protozoa grow submaximally at prey Fe:C ratios <15 μmol mol^{-1} (Fig. 1). Such

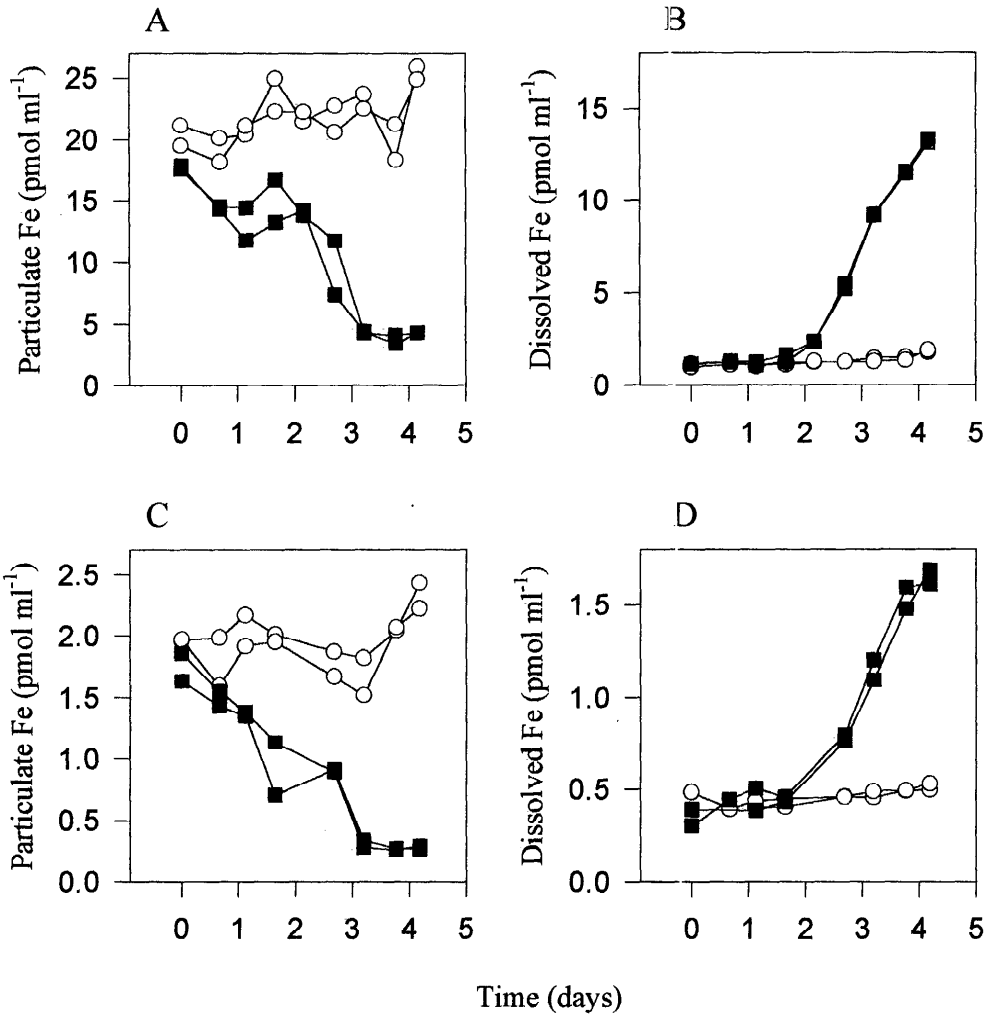

Fig. 4. Time course of iron dynamics in cultures with bacteria and *Paraphysomonas imperforata* (■; replicates shown) and control cultures with bacteria alone (○; replicates shown). Particulate (A) and dissolved (B) Fe in the high-iron treatment. Particulate (C) and dissolved (D) Fe in the low-iron treatment.

slow growth rates were obtained solely by variation in prey iron content, because prey biomass (C) was constant over the range of iron treatments. Growth limitation by iron can thus be induced in phagotrophic protozoa. An important issue, however, is whether this limitation is the direct result of iron deficiency in the protozoa or an indirect effect of low iron on their bacterial prey.

In the pFe21 growth medium used to cultivate iron-poor bacteria, both strains were growth-rate limited, whereas iron-rich bacteria grew at maximum rates at pFe18 (Tortell et al. 1996). Thus, if iron limitation altered the bacteria in other ways, iron content might not be the only difference between the two types of prey. Morphological and structural changes to algae and bacteria, for example, are known to be induced by nutrient deficiency and to reduce their digestibility (González et al. 1993; van Donk and Hessen 1993). Although they might influence consumer growth, such indirect effects of iron are not likely to have been important in our experiments. We observed elongation of some bacteria in the Jul88 cultures maintained in low-iron medium, but no morphological changes were observed in Tef2, which elicited the same iron-induced growth reduction in the protozoa (Fig. 1). Neither strain showed any obvious difference in aggregation under low-iron conditions, but this was not assessed quantitatively.

Biochemical changes that accompany nutrient limitation may also influence prey nutritional quality. Indeed, what seems to be phosphorus limitation of *Daphnia* is more a consequence of the low levels of eicosapentaenoic acid than of low P content in P-limited algal prey (Müller-Navarra 1995). Although we know the bulk chemical content of the prey bacteria (C:N) was not affected by iron, a large and unspecified list of potential differences exists between iron-sufficient and iron-deficient bacteria. We thus addressed the issue of mineral vs. biochemical limitation by comparing growth of protozoa fed iron-poor prey with and without added surface-bound iron. Because the results showed that growth of *P. imperforata* was significantly faster in the for-

Table 2. Carbon budget for *Paraphysomonas imperforata* consuming live and heat-killed, iron-rich (pFe18-grown) or iron-poor (pFe21-grown) bacterial prey (strain Jul88). The gross carbon growth efficiency (GCGE) was calculated as (growth/ingestion) × 100, and the assimilation efficiency (CAE) as (ingestion − excretion)/ingestion × 100. Means are based on two replicates that differed by <7% on average.

	Growth conditions			
	High iron		Low iron	
Parameter	Live prey	Heat-killed prey	Live prey	Heat-killed prey
Initial bacterial C (mM)	0.19	0.14	0.29	0.19
Ingestion (pmol C prot^{-1} d^{-1})	1.4	1.3	2.1	2.0
Growth (pmol C prot^{-1} d^{-1})	0.51	0.41	0.39	0.26
CO_2 evolution (pmol C prot^{-1} d^{-1})	0.8[1]	0.80	1.4[1]	1.50
Excretion (pmol C prot^{-1} d^{-1})	0.11	0.11	0.34	0.53
GCGE (%)	36	33	18	13
CAE (%)	92	91	84	73
CO_2/I (%)	56	63	66	79

[1] Calculated by difference.

Table 3. Iron budget for *Paraphysomonas imperforata* consuming iron-rich (pFe18-grown) or iron-poor (pFe21-grown) bacterial prey (strain Jul88). The gross iron growth efficiency (GFeGE) was calculated in the same way as GCGE. Iron regeneration efficiency (FeRE) equals (excretion/ingestion) × 100. Means are based on two replicates that differed by <8% on average.

	Growth conditions	
Parameter	High iron	Low iron
Initial bacterial Fe (nM)	17.7	1.8
Ingestion (amol Fe prot^{-1} d^{-1})	110	16
Growth (amol Fe prot^{-1} d^{-1})	28	2.0
Excretion (amol Fe prot^{-1} d^{-1})	64	12
GFeGE (%)	26	14
FeRE (%)	58	84

mer case, growth rate reduction in the protozoa fed iron-poor prey seems to be caused by direct elemental limitation by iron.

The metabolic signature of the slow-growing protozoa provided further support for direct iron limitation. Protozoan ingestion rates would be expected to decrease if iron-poor bacteria were indigestible or difficult to capture. However, ingestion rates increased, and slower growth was a result of lower growth efficiency (Table 2). The ~50% decrease in GCGE of *Paraphysomonas* in low-iron cultures was reflected in a dramatic decline in the activity of the ETS. Because it contains the bulk of the iron in a heterotrophic cell, reduced ETS activity under low-iron conditions was anticipated. Electron transport system reduction seems to be a specific consequence of iron deficiency, because the metabolic reactions that maintain filtration rates, for example, were not similarly downregulated.

Taken together, the three lines of evidence presented above—the relationship between protozoan growth rate and bacterial Fe:C, the stimulation of growth by iron-coated bacteria, and the biochemistry of growth limitation—suggest the marine protozoa in our experiments experienced elemental iron limitation. The question naturally arises of whether this is simply an interesting laboratory result or whether heterotrophic flagellates could be limited by iron in the ocean. Because protozoa are apparently not able to use dissolved iron for growth, their potential for iron limitation should depend entirely on the iron content of their food. A low Fe:C of 9 μmol mol^{-1} in the bacterial size fraction (0.2–1 μm) of the open subarctic Pacific (Tortell et al. 1996) suggests their food could be iron-poor. Indeed, as it falls within the range of prey Fe:C found here to inhibit growth, heterotrophic flagellates and other protozoa may well experience iron deficiency in parts of the sea. Although this speculation clearly awaits confirmation in the field, and may depend on in situ prey abundance (Sterner and Robinson 1994; Rothhaupt 1995) or on the types of prey items naturally consumed by protozoa, it offers another explanation for the observation that microheterotroph biomass increases following iron addition in bottle incubations (Buma et al. 1991; Chavez et. al. 1991) and mesoscale fertilization experiments (Martin et al. 1994).

Iron quotas—Iron quotas of the protozoa measured under low-iron conditions were higher than those of phytoplankton (Maldonado and Price 1996) and a number of marine heterotrophic bacteria (Tortell et al. 1996). This result is perhaps surprising, because a heterotrophic mode of existence lacks the iron-dependent photosynthetic reactions that are known to incur a high demand for iron in photoautotrophs. However, the ETS redox proteins needed to maintain active heterotrophic metabolism can impart a substantial iron requirement. Indeed, in iron-limited bacteria, where most cellular Fe is associated with the ETS (Righelato 1969; Light and Clegg 1974; Granger and Price in prep.), iron quotas are relatively high (Tortell et al. 1996). Assuming that all heterotrophs have similar respiratory pathways, we expected protozoa to have minimum iron quotas similar to or less than those of bacteria. Their quotas would most likely be lower, because the specific respiration rates (respiration/biomass), and hence ETS/biomass, of heterotrophs decrease with increasing size (Peters 1983). Iron should thus be "demagnified" as it passes up the food chain. Our results, however, seem to run counter to this allometric argument, because the flagellates in the low-iron experiments had higher iron quotas than did their prey. This may be a consequence of sample size, since only two species of a single genus were examined, or a consequence of scale, since the allometric relationship holds best when considering organisms that differ in size by many orders of magnitude. From a compilation of early measurements (Vinogradov 1953) we find a mean Fe:C in marine fish of 4.5 μmol Fe:mol C (median = 3, n = 72; assuming wet wt = 5 × dry wt). This lends support to the idea of iron demagnification. The data are difficult to interpret, however, because the iron nutritional status of the large organisms is not known. An alternative explanation for the high quotas is that eukaryotic metabolism is relatively more iron-costly than prokaryotic metabolism, or it uses large amounts of iron not associated with the ETS. Indeed, when we consider bacteria, protozoa, and zooplankton, we

Table 4. Electron transport system activity (ETS) normalized to cellular Fe in marine heterotrophs. A range in size is shown when data for multiple species were averaged. Bacterial data are from Tortell et al. (1996). Zooplankton ETS activity and dry weight were taken from King and Packard (1975), and Fe quotas were calculated from Martin and Knauer (1973) assuming C = 0.4×dry wt.

Organism	Size (μmol C ind.$^{-1}$)	Fe:C (μmol mol^{-1})	ETS/Fe (ml O_2 h^{-1} μmol Fe^{-1})
Bacteria			
Iron-deficient	$0.40–3.0\times10^{-8}$	7.5±1.7	$8.8\pm1.4\times10^{3}$
Iron-sufficient	$0.40–2.0\times10^{-8}$	56±11	$1.3\pm0.15\times10^{3}$
Protozoa			
Paraphysomonas imperforata			
Iron-deficient	2.4×10^{-7}	8.2±0.1	$2.7\pm0.45\times10^{2}$
Iron-sufficient	2.4×10^{-7}	98±3.0	$1.8\pm0.44\times10^{2}$
Zooplankton			
Copepods			
Euphausia pacifica	0.03–6.0	16±6.0	4.0±0.8
	1.9×10^{2}	8.0±4.0	4.0±2.0

find a dramatic decrease in the ratio of ETS to Fe (Table 4), suggesting a greater importance of non-ETS iron in larger organisms.

Carbon and nitrogen metabolism—Iron limitation profoundly affected carbon metabolism in *P. imperforata*. These protozoa converted less prey C into biomass and released more ingested C as DOC and CO_2, compared to those consuming iron-rich prey. The validity of these results rests on the equal fulfillment in both iron treatments of assumptions made in calculating GCGE. Most important among these, we assumed that at the end of the flagellate growth interval POC consisted entirely of protozoa and uneaten bacteria. GGEs determined from measurements of protozoan volume are ~12% lower than those measured by the method we used (Fenchel 1982; Caron et al. 1985; Geider and Leadbeater 1988). Presumably the discrepancy exists because some ingested C is egested as unincorporated POC (*see* Stoecker 1984). If this egested C is retained by the filters, it would be counted as protozoan biomass and would thus increase the measured G, so that CO_2 evolution calculated by difference ($CO_2 = I - G - E$) would be lower than CO_2 evolution measured directly. Because the ratio of CO_2 measured to CO_2 calculated in the CO_2 evolution experiment was 1.08 and 1.27 for the iron-rich and iron-poor treatments, overestimation of GCGE was, if anything, more severe in the low-iron treatment. Thus, we think that the observed differences in C metabolism between Fe treatments are real.

The ammonium excretion results showed that N metabolism was also affected by iron status. Lower NH_4^+ regeneration efficiencies of iron-limited protozoa implies that they excreted more of their ingested N as DON or urea, or accumulated more N in biomass. An increased N content of the protozoa seems unlikely, however, because C per protozoan was the same in both iron treatments, and C:N ratios of other plankton are known to be independent of iron (Maldonado and Price 1996; Tortell et al. 1996). Because UV irradiation inhibited bacterial replication but not respiration, it is possible that the prey were able to take up and accumulate N. Such secondary uptake is unlikely to have occurred, however, because the 14 μM of NH_4^+ present in both the high- and low-iron control cultures at the time of protozoan inoculation was not consumed by the UV-killed bacteria during the experiment. If we thus rule out accumulation of N in the protozoa or bacteria, the mass balance suggests that when the protozoa consumed iron-poor prey, the excess N that they ingested was excreted as DON.

A modestly speculative interpretation of these data provides the following working model of iron-limited metabolism of protozoa: Iron deficiency induces increased protozoan filtration rates to maximize ingestion. However, under low-iron conditions, insufficient iron is assimilated to support rapid rates of electron transport by the ETS so that energy extraction (adenosine 5′-triphosphate [ATP] production) from the C ration is inhibited. Curiously, more CO_2 is evolved by these ETS-inhibited cells, as observed in marine bacteria (Tortell et al. 1996), suggesting they have a greater reliance on substrate-level pathways to generate ATP, or that they process more C through the TCA cycle. The latter scenario is difficult to envisage, as it would presumably result in excess production and accumulation of reductant. Cellular feedback mechanisms mediated by iron stress increase the portion of the ingested C and N ration released by the protozoa. In this model, iron-limited protozoa have lower ammonium regeneration efficiencies because less of the N ration is assimilated, and only this fraction undergoes deamination.

Iron assimilation and regeneration—The GFeGEs reported here for *P. imperforata* are very similar to those of metazoan grazers (7–25%; Hutchins and Bruland 1994; Hutchins et al. 1995). One of the most surprising results in this regard was the importance of the iron content of the prey: Flagellates assimilated considerably less iron (2×) from the iron-poor bacteria, despite being limited by the element (Table 3). This is in striking contrast to studies of N and P regeneration, which generally find reduced regeneration efficiency for an element by protozoa when prey are deficient in that element (Goldman and Caron 1985; Goldman et al. 1987; however, *see* Eccleston-Parry and Leadbeater [1995], who found no effect of prey nutritional quality on protozoan nutrient regeneration).

The assumptions made in the calculation of GCGE apply equally to the calculation of GFeGE. We also assumed that if the live bacterial prey reassimilated some of the regenerated Fe, they did so to the same extent in both iron treatments. The good accordance between GCGE measured with live and heat-killed bacteria suggests that reassimilation of C did not occur. Reassimilation of iron would lead to an underestimation of I and an overestimation of G (as remaining bacteria accumulate iron relative to the controls), with the net effect that GFeGE would be overestimated. Greater GFeGE observed in the high-iron treatment could thus be explained if bacterial assimilation of excreted Fe was greater under these conditions. Such secondary uptake, however, is more likely to be greater in the low-iron treatment, where the bacteria have presumably maximized their iron uptake systems.

An alternative way to evaluate the validity of the iron results is to look at their internal consistency. It should be that

$$\text{Fe}:\text{C}_{\text{flagellate}} = \text{Fe}:\text{C}_{\text{bacteria}} \times \text{GFeGE/GCGE}, \quad (7)$$

where GFeGE and GCGE refer to the flagellate. We find that the right-hand side of this relationship exceeds the left-hand side by ~14% for both low- and high-iron treatments. This suggests that while there are some methodological inconsistencies, they act equally in both treatments. We are thus confident that the problems of reassimilation and particulate egestion do not confound our interpretation of the data.

A biological explanation for the paradoxical result of lower GFeGE from iron-poor bacteria may be that these prey contain relatively large pools of nonassimilable Fe. Price (1968) proposed that the order in which cellular iron pools are lost as iron limitation proceeds reflects the strength of cellular iron chelates, so that severely iron-limited plant cells retain only that which is most tightly bound. Although this model has yet to be confirmed, bacteria grown with excess iron are known to produce soluble iron storage proteins such as bacterioferritin (Harrison et al. 1980; Perry et al. 1993) and contain relatively more non-heme Fe (Righelato 1969; Light and Clegg 1974; Archibald and DeVoe 1978) than do iron-limited cells. Such chemical forms may be less available for biological assimilation. During preliminary investigations into iron partitioning in strain Jul88, we found that the iron of iron-replete cells was more reactive toward glass beads than was that of iron-deplete cells (data not shown).

Cellular partitioning of iron within prey cells might also affect protozoan assimilation, as it does with metazoan grazers (Reinfelder and Fisher 1991; Hutchins et al. 1995). This may explain the difference between the pattern of regeneration observed here for iron (greater efficiency when prey are iron-poor) and the results obtained for N and P regeneration (Goldman and Caron 1985; Goldman et al. 1987). Perhaps the relative distribution of trace metals within prey cells is more sensitive to prey nutritional status than is major nutrient distribution, or, alternatively, the assimilation of trace metals by grazers may be more dependent on the cellular forms of the nutrient. Another possibility is that under iron stress the ability of protozoans to transport all materials across the food vacuole membranes is decreased, leading to high Fe regeneration efficiencies. Clearly, the factors that regulate metal assimilation by protozoa in general, and their possible interaction with prey nutritional status in particular, deserve further attention. For example, phytoplankton, although iron-poor, might provide a good source of dietary Fe if their cellular pools are more easily assimilated than are those of bacteria.

Remineralization of cellular Fe is thought to be a key process in the surface-water biogeochemistry of iron (Bruland et al. 1991; Hutchins et al. 1993). We observed very high maximum iron regeneration efficiencies for *P. imperforata* consuming bacterial prey (59 and 84% for iron-replete and iron-deficient prey). Coupled with the large amount of iron in the bacterial community (Tortell et al. 1996), this result suggests that protozoan bactivory is a potentially important source of regenerated Fe. However, the chemical nature and reactivity of this iron, and hence its availability to phytoplankton and bacterioplankton, is unknown. Some regenerated metals may not be immediately available for phytoplankton use (Twiss and Campbell 1995). Indeed, the transience of the biological (phytoplankton) response to large-scale iron addition (Martin et al. 1994; Coale et al. 1996) speaks against rapid and efficient recycling of cellular Fe in these parts of the sea.

This paper documents the first investigation of iron limitation in heterotrophic marine protozoa. *P. imperforata* and *P. butcheri* have relatively high cellular iron requirements and grow slowly when fed iron-poor bacterial prey. Under low-iron conditions, these protozoa have lower GCGEs, excrete more of their ingested ration as DOC and DON, and regenerate less NH_4^+. Protozoa in iron-poor waters may thus be less efficient at converting bacterial prey into biomass, thereby affecting the role of the microbial loop as a remineralization pathway vs. a link to higher trophic levels. Collectively, the results suggest that the concept of iron limitation can be extended to heterotrophic grazers, and imply that the entire ecology of oceanic regions could be modulated by the supply and availability of iron.

References

ARCHIBALD, I. S., AND I. W. DEVOE. 1978. Iron in *Neisseria meningitidis*: Minimum requirements, effects of limitation, and characteristics of uptake. J. Bacteriol. **136:** 35–48.

BARBEAU, K., J. W. MOFFETT, D. A. CARON, P. L. CROOT, AND D. L. ERDNER. 1996. Role of protozoan grazing in relieving iron limitation of phytoplankton. Nature **380:** 61–63.

BRULAND, K. W., J. R. DONAT, AND D. A. HUTCHINS. 1991. Interactive influences of bioactive trace metals on biological production in oceanic waters. Limnol. Oceanogr. **36:** 1555–1577.

BUMA, A. G. J., H. J. W. DE BAAR, R. F. NOLTING, AND A. J. VAN BENNEKOM. 1991. Metal enrichment experiments in the Weddell-Scotia seas: Effects of Fe and Mn on various plankton communities. Limnol. Oceanogr. **36:** 1865–1878.

CARON, D. A., AND J. C. GOLDMAN. 1990. Protozoan nutrient regeneration, p. 283–306. *In* G. M. Caprulio [ed.], Ecology of marine protozoa. Oxford.

———, ———, O. K. ANDERSON, AND M. R. DENNETT. 1985. Nutrient cycling in a microflagellate food chain: II. Population dynamics and carbon cycling. Mar. Ecol. Prog. Ser. **24:** 243–254.

CHAVEZ, F. P., AND OTHERS. 1991. Growth rates, grazing, sinking, and iron limitation of equatorial Pacific phytoplankton. Limnol. Oceanogr. **36:** 1816–1833.

COALE, K. H., AND OTHERS. 1996. A massive phytoplankton bloom induced by an ecosystem-scale iron fertilization experiment in the equatorial Pacific Ocean. Nature **383:** 495–501.

CULLEN, J. J., M. R. LEWIS, C. O. DAVIS, AND R. T. BARBER. 1992. Photosynthetic characteristics and estimated growth rates indicate grazing is the proximate control of primary production in the equatorial Pacific. J. Geophys. Res. **97:** 639–654.

ECCLESTON-PARRY, J. D., AND B. S. C. LEADBEATER. 1995. Regeneration of phosphorus and nitrogen by four species of heterotrophic nanoflagellates feeding on three nutritional states of a single bacterial strain. Appl. Environ. Microbiol. **61:** 1033–1038.

FENCHEL, T. 1982. Ecology of heterotrophic microflagellates. II. Bioenergetics and growth. Mar. Ecol. Prog. Ser. **8:** 225–231.

GEIDER, J. R., AND B. S. C. LEADBEATER. 1988. Kinetics and energetics of growth of the marine choanoflagellate *Stephanoeca diplocostata*. Mar. Ecol. Prog. Ser. **47:** 169–177.

GOLDMAN, J. C., AND D. A. CARON. 1985. Experimental studies on an omnivorous microflagellate: Implications for grazing and nutrient-regeneration in the marine microbial-food-chain. Deep-Sea Res. **32:** 899–915.

———, ———, AND M. R. DENNETT. 1987. Nutrient cycling in a microflagellate food chain: IV. Phytoplankton–microflagellate interactions. Mar. Ecol. Prog. Ser. **38:** 75–87.

GONZÁLEZ, J. M., E. B. SHERR, AND B. F. SHERR. 1993. Differential feeding by marine flagellates on growing versus starving, and on motile versus nonmotile, bacterial prey. Mar. Ecol. Prog. Ser. **102:** 257–276.

HARRISON, P. M., A. G. CLEGG, AND K. MAY. 1980. Ferritin structure and function, p. 131–171. *In* A. Jacobs and M. Worwood [eds.], Iron in biochemistry and medicine. II. Academic.

HESSEN, D. O. 1992. Nutrient element limitation of zooplankton production. Am. Nat. **140:** 799–814.

HUDSON, R. J. M., AND F. M. M. MOREL. 1989. Distinguishing between extra- and intracellular iron in marine phytoplankton. Limnol. Oceanogr. **34:** 1113–1120.

HUTCHINS, D. A., AND K. W. BRULAND. 1994. Grazer-mediated regeneration and assimilation of Fe, Zn and Mn from planktonic prey. Mar. Ecol. Prog. Ser. **110:** 259–269.

———, G. R. DITULLIO, AND K. W. BRULAND. 1993. Iron and regenerated production: Evidence for biological iron recycling in two marine environments. Limnol. Oceanogr. **38:** 1242–1255.

———, W.-X. WANG, AND N. S. FISHER. 1995. Copepod grazing and the biogeochemical fate of diatom iron. Limnol. Oceanogr. **40:** 989–994.

KENNER, R. A., AND S. I. AHMED. 1975. Correlation between oxygen utilization and electron transport activity in marine phytoplankton. Mar. Biol. **33:** 129–133.

KING, F. D., AND T. T. PACKARD. 1975. Respiration and the respiratory electron transport activity in marine zooplankton. Limnol. Oceanogr. **20:** 849–854.

LIGHT, P. A., AND R. A. CLEGG. 1974. Metabolism in iron-limited growth, p. 35–64. *In* J. B. Neilands [ed.], Microbial iron metabolism: A comprehensive treatise. Academic.

MALDONADO, M. T., AND N. M. PRICE. 1996. Influence of N substrate on Fe requirements of marine centric diatoms. Mar. Ecol. Prog. Ser. **141:** 161–172.

MARTIN, J. H., AND OTHERS. 1994. Testing the iron hypothesis in ecosystems of the equatorial Pacific ocean. Nature **371:** 123–130.

———, AND S. E. FITZWATER. 1988. Iron deficiency limits phytoplankton growth in the north-east Pacific subarctic. Nature **331:** 341–343.

———, AND G. A. KNAUER. 1973. The elemental composition of plankton. Geochim. Cosmochim. Acta **37:** 1639–1653.

MICHAELS, A. F., AND M. W. SILVER. 1988. Primary production, sinking fluxes and the microbial food web. Deep-Sea Res. **35:** 473–490.

MÜLLER-NAVARRA, D. C. 1995. Biochemical versus mineral limitation in *Daphnia*. Limnol. Oceanogr. **40:** 1209–1214.

OLSEN, Y., A. JENSEN, H. REINSTREN, K. Y. BORSHEIM, M. HELDAL, AND A. LANGELAND. 1986. Dependence of the rate of release of phosphorus by zooplankton on the C:P ratio in the food supply, as calculated by a recycling model. Limnol. Oceanogr. **31:** 34–44.

PACKARD, T. T., AND P. J. B. WILLIAMS. 1981. Rates of respiratory oxygen consumption and electron transport in surface seawater from the northwest Atlantic Ocean. Oceanol. Acta **4:** 351–358.

PAKULSKI, J. D., AND OTHERS. 1996. Iron stimulation of Antarctic bacteria. Nature **383:** 133–134.

PARSONS, T. R., Y. MAITA, AND C. M. LALLI. 1984. A manual of chemical and biological methods for seawater analysis. Pergamon.

PERRY, R. D., T. S. LUCIER, D. J. SIKKEMA, AND R. R. BRUBAKER. 1993. Storage reservoirs of hemin and inorganic iron in *Yersinia pestis*. Infect. Immunol. **61:** 32–39.

PETERS, R. H. 1983. The ecological implications of body size. Cambridge.

PORTER, K. G., AND Y. S. FEIG. 1980. The use of DAPI for identifying and counting aquatic microflora. Limnol. Oceanogr. **25:** 943–948.

PRICE, C. A. 1968. Iron compounds and plant nutrition. Ann. Rev. Plant Physiol. **19:** 239–248.

PRICE, N. M., B. A. AHNER, AND F. M. M. MOREL. 1994. The equatorial Pacific Ocean: Grazer-controlled phytoplankton populations in an iron-limited ecosystem. Limnol. Oceanogr. **39:** 520–534.

———, L. F. ANDERSEN, AND F. M. M. MOREL. 1991. Iron and nitrogen nutrition of equatorial Pacific plankton. Deep-Sea Res. **38:** 1361–1378.

———, AND P. J. HARRISON. 1987. Comparison of methods for the analysis of dissolved urea in seawater. Mar. Biol. **94:** 307–317.

———, ———, J. G. HERING, AND OTHERS. 1988–1989. Preparation and chemistry of the artificial algal culture medium Aquil. Biol. Oceanogr. **6:** 443–461.

RAVEN, J. 1988. The iron and molybdenum use efficiency of plant growth with different energy, carbon and nitrogen sources. New Phytol. **109:** 1–18.

REINFELDER, J. R., AND N. S. FISHER. 1991. The assimilation of elements ingested by marine copepods. Science **251:** 794–796.

RIGHELATO, R. C. 1969. The distribution of iron in iron-deficient toxin-synthesizing and in excess-iron non-toxin-synthesizing *Cornybacterium diptheriiae*. J. Gen. Microbiol. **58:** 411–419.

ROTHHAUPT, K. O. 1995. Algal nutrient limitation affects rotifer growth rate but not ingestion rate. Limnol. Oceanogr. **40:** 1201–1208.

STERNER, R. W., J. ELSER, AND D. O. HESSEN. 1992. Stochiometric relationships among producers, consumers and nutrient cycling in pelagic ecosystems. Biogeochemistry **17:** 49–67.

STERNER, R. W., AND J. L. ROBINSON. 1994. Thresholds for growth in *Daphnia magna* with high and low phosphorus diets. Limnol. Oceanogr. **39:** 1228–1232.

STOECKER, D. K. 1984. Particle production by planktonic ciliates. Limnol. Oceanogr. **29:** 930–940.

STROM, S. L., AND N. A. WELSCHMEYER. 1991. Pigment-specific rates of phytoplankton growth and microplankton grazing in the open subarctic Pacific Ocean. Limnol. Oceanogr. **36:** 50–63.

SUNDA, W. G., D. G. SWIFT, AND S. A. HUNTSMAN. 1991. Low iron requirement for growth in oceanic phytoplankton. Nature **351:** 55–57.

TORTELL, P. D., M. T. MALDONADO, AND N. M. PRICE. 1996. The importance of heterotrophic bacteria in Fe-limited ocean ecosystems. Nature **383:** 330–332.

TWISS, M. R., AND P. G. C. CAMPBELL. 1995. Regeneration of trace metals from picoplankton by nanoflagellate grazing. Limnol. Oceanogr. **40:** 1418–1429.

UDENFRIEND, S., S. STEIN, P. BÖHLEN, W. DAIRMAN, W. LEIMGRUBER, AND M. WEIGLE. 1972. Fluorescamine: A reagent for assay of amino acids, peptides, proteins, and primary amines in the picomole range. Science **178:** 871–873.

URABE, J., AND Y. WANATABE. 1992. Possibility of N or P limitation for planktonic cladocerans: An experimental test. Limnol. Oceanogr. **37:** 244–251.

VAN DONK, E., AND D. O. HESSEN. 1993. Grazing resistance in nutrient-stressed phytoplankton. Oecologia **93:** 508–511.

VINOGRADOV, A. P. 1953. The elementary chemical composition of marine organisms. Sears Foundation for Marine Research. Memoir II.

WESTALL, J. C., J. L. ZACHARY, AND F. M. M. MOREL. 1976. MINEQL: A computer program for the calculation of chemical equilibrium composition of aqueous systems. Mass. Inst. Technol. R. M. Parsons Lab. Tech. Note 18.

Received: 27 August 1996
Accepted: 19 June 1997
Amended: 27 June 1997